

Accepted Manuscript

Synthesis and biological evaluation of 5,10-Dihydro-11*H*-dibenzo[*b,e*]
[1,4]diazepin-11-one structural derivatives as anti-cancer and apoptosis inducing
agents

Chintakunta Praveen Kumar, T. Srinivasa Reddy, Prathama S. Mainkar, Vipul Bansal,
Ravi Shukla, Srivari Chandrasekhar, Helmut M. Hügel

PII: S0223-5234(15)30391-3

DOI: [10.1016/j.ejmech.2015.12.007](https://doi.org/10.1016/j.ejmech.2015.12.007)

Reference: EJMECH 8247

To appear in: *European Journal of Medicinal Chemistry*

Received Date: 20 August 2015

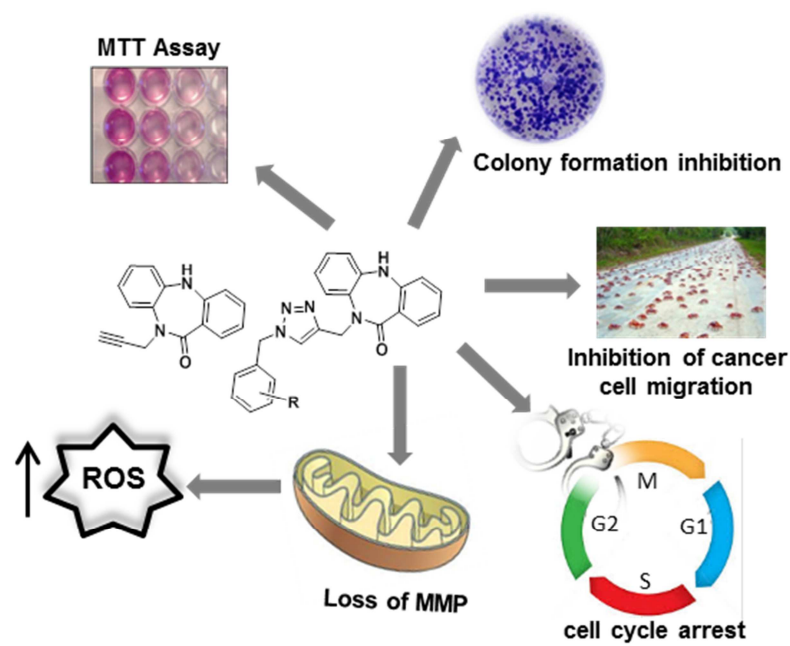
Revised Date: 19 November 2015

Accepted Date: 2 December 2015

Please cite this article as: C.P. Kumar, T.S. Reddy, P.S. Mainkar, V. Bansal, R. Shukla, S. Chandrasekhar, H.M. Hügel, Synthesis and biological evaluation of 5,10-Dihydro-11*H*-dibenzo[*b,e*] [1,4]diazepin-11-one structural derivatives as anti-cancer and apoptosis inducing agents, *European Journal of Medicinal Chemistry* (2016), doi: 10.1016/j.ejmech.2015.12.007.

This is a PDF file of an unedited manuscript that has been accepted for publication. As a service to our customers we are providing this early version of the manuscript. The manuscript will undergo copyediting, typesetting, and review of the resulting proof before it is published in its final form. Please note that during the production process errors may be discovered which could affect the content, and all legal disclaimers that apply to the journal pertain.





Synthesis and biological evaluation of 5,10-Dihydro-11H-dibenzo[b,e][1,4]diazepin-11-one structural derivatives as anti-cancer and apoptosis inducing agents

Chintakunta Praveen Kumar^{a,b,c}, T. Srinivasa Reddy^{a,d,e,f}, Prathama S. Mainkar^c, Vipul Bansal^{a,d,e}, Ravi Shukla^{a,d,e,f}, Srivari Chandrasekhar^{c*}, Helmut M. Hugel^{a*}

^a*School of Applied Sciences, RMIT University, Melbourne 3001, Australia*

^b*IICT-RMIT Research Centre SIR-Indian Institute of Chemical Technology, Hyderabad 500 007, India*

^c*Division of Natural Products Chemistry, CSIR-IICT, Hyderabad 500 007, India*

^d*Health Innovations Research Institute, RMIT University, Melbourne 3083, Australia*

^e*Ian Potter NanoBioSensing Facility, NanoBiotechnology Research Laboratory, School of Applied Sciences, RMIT University, Melbourne 3000, Australia*

^f*Centre for Advanced Materials and Industrial Chemistry, RMIT University, Melbourne 3000, Australia*

*Corresponding authors:

Associate Prof. Helmut M. Hugel

School of Applied Sciences, RMIT University
GPO Box 2476, Melbourne 3001 VIC Australia
E-mail: helmut.hugel@rmit.edu.au
Tel: +61 3 9925 2626

Dr. S. Chandrasekhar

Director
CSIR-Indian Institute of Chemical Technology,
Tarnaka, Hyderabad, India-500 007
E-mail: srivaric@iict.res.in
Fax: +91-40-27160512

Abstract

A series of thirteen 5*H*-dibenzo [*b,e*][1,4]diazepin-11(10*H*)-one structural derivatives has been synthesized and evaluated for anti-proliferative activity against five human cancer cell lines. Compound **9a** exhibited potent tumour growth inhibition in all cell lines with IC₅₀ values in the range of 0.71-7.29 μ M. Experiments on lung (A549) and breast (MDAMB-231) cancer cell lines to investigate the mechanisms of growth inhibition and apoptosis inducing effects of **9a** showed that it arrested both cancer cell lines in the G2/M phase of cell cycle in a dose dependent manner. Hoechst staining analysis revealed that **9a** inhibited tumour cell proliferation through apoptosis induction. Additionally, the mitochondrial membrane potential ($\Delta\Psi_m$) was affected and the levels of reactive oxygen species (ROS) were raised. The simple synthetic preparation and their biological properties make these dibenzodiazepinone-triazole scaffolds promising new entities for the development of cancer therapeutics.

Key words

Dibenzodiazepinones; triazoles; anti-cancer activity; apoptosis

1.0 Introduction

Cancer is the leading global health burden that at some time will directly or indirectly affect the lives of most people. Local cancer treatments, such as surgical and radiation therapies are not always viable due to the position of the tumour in the body. Furthermore, these methods are often unsuccessful in completely removing tumours. Chemotherapy is a systemic cancer treatment and chemotherapeutic drugs interfere with the cell cycle and thus cell division, angiogenesis or induce tumour cell apoptosis by several signalling pathways. However, due

to the high cancer mortality rate, development of drug resistance and undesirable side effects there is an urgent need to design and synthesise new anti-cancer drugs.

The dibenzodiazepinone [5,10-dihydro-11*H*-dibenzo[*b,e*][1,4]diazepin-11-one]**1**(Figure 1) scaffold is known to exhibit wide range of biological activities including neuroleptic [1], anti-inflammatory [2], anti-depressant [3], anti-microbial [4], anti-hypertensive [5] and anti-viral [6] efficacies. Moreover, dibenzodiazepinone research led to the discovery of drug leads such as Chk1 kinase inhibitors **2** (Figure 1) [7] and the histone deacetylase HDAC [8] inhibitor **3**. Diazepinomicin **4** is an unusual farnesylated-dibenzodiazepinone secondary metabolite isolated [3, 9] from *Micromonospora* and contains dibenzodiazepinone skeleton that is unprecedented among natural products and its biosynthesis [10] has been described recently. The anti-tumour, anti-bacterial and anti-inflammatory activities of **4** have also been reported [11]. Compound **4** (Figure 1) induces apoptosis by selectively targeting the peripheral benzodiazepine receptor (PBR) [12].

<Figure 1>

On the other hand, many triazole containing compounds exhibit extensive range of pharmacological activities including potent anticancer properties [13]. For instance, cefatrizine, tazobactam and carboxyamidotriazole are some of the triazole containing compounds which are in clinical or preclinical studies [14, 15]. Among the triazoles, 1,2,3-triazoles are capable of interacting with the biological targets through *H*-bonding and are stable to metabolic degradation [16]. Based on these observations and inspired by the promising anticancer activities of dibenzodiazepinones and 1,2,3-triazoles, we designed a series of dibenzodiazepinone-triazole hybrid compounds with a view to produce promising anticancer agents.

The diverse therapeutic application of dibenzodiazepine derivatives and related compounds in medicinal chemistry has stimulated considerable synthesis interest in the construction of this tricyclic ring privileged scaffold. Eight chemical retro synthetic approaches are presented in Figure 2. In 1985, a one-step synthesis delivered in a modest 30% yield the dibenzodiazepine scaffold [17, 18] by refluxing 2-chlorobenzoic acid and *o*-phenyldiamine in the presence of copper as catalyst and chlorobenzene as solvent that is denoted as route I. The reaction product from 2-iodoaniline and a substituted 1-fluoro-2-nitrobenzene was then employed in a palladium mediated intramolecular carbonylation reaction [19] to provide the 1,4-benzodiazepine product identified as route II. The ring closing reductive lactamization methodology [20] using the dissolving-metal condition of iron and acetic acid was another synthesis approach [route III]. The amine ring closure path gave an efficient synthesis of 1,4-benzodiazepines [21] via the double amination of ortho-substituted aryl bromides is shown as route IV. The one step preparation of dibenzodiazepines [22] and related derivatives illustrated as route V was accomplished by the palladium-catalyzed reaction between alkyl 2-(2-chlorophenylamino)benzoate and ammonia. The utilization of POCl₃ enabled substituted ethyl 2-(phenylamino)phenylcarbamate to participate in an intramolecular lactamization *via* the electrophilic aromatic substitution to furnish route VI to the desired 1,4-benzodiazepine [23]. The synthesis of the target compound was also achieved through a high temperature, Cs₂CO₃ driven, double nucleophilic aromatic substitution reaction [24] of anthranilamide with 2,5-dichloronitrobenzene depicted as route VII. Recently, route VIII, the 1,4-benzodiazepine core [25] structure was assembled from the substituted *N*-methoxy-2-(methylphenylamino)benzamide through an intramolecular PIDA-mediated oxidative C-N bond synthesis in 82% yield in this cyclisation step.

<Figure 2>

2.0 Results and Discussion

2.1 Chemistry

We utilized a slightly modified one step dibenzodiazepine synthesis [route I in Figure 2]. Our dibenzodiazepinone-triazole analogues were prepared following the reaction sequence depicted in Scheme 1. Initially, ethyl-2-iodobenzoate **5** was reacted with *o*-phenylenediamine **6** in presence of 10 mol% CuI in a pressure tube at 100 °C to give the dibenzodiazepinone **1** in 50% yield [26]. Propargylation of **1** was first carried out with propargyl bromide and NaH in anhydrous THF solvent at ice-bath temperature. But, these conditions did not afford the required compound **7** (Scheme 1). When, the reaction was carried out with *n*-BuLi at -20 °C in freshly distilled THF, the desired N-propargylated compound was obtained in 72% yield. Decreasing the reaction temperature to -78 °C did not improve the reaction yield.

<Scheme 1>

The formation of product **7** was evident from ¹H NMR and ¹³C NMR spectroscopy. Then, **7** was subjected to click reaction conditions to construct the 1,2,3-triazole ring. Various benzyl azides **8a-k** used in the reaction were prepared from respective aldehydes following literature procedures [27]. Azides underwent 3+2 cycloaddition (CuAAC) with **7** in presence of CuSO₄·5H₂O and sodium ascorbate in *t*BuOH/H₂O (1:1) to give triazole-products **9a-k** (Scheme1). Formation of triazole ring was determined by the characteristic singlet in the aromatic region in ¹H, by peak at around 120 ppm in ¹³C NMR, and from mass spectral analysis.

2.2 Biological studies

2.2.1 *In vitro* cytotoxic activity

All the synthesised dibenzodiazepinone-triazole derivatives were screened for their anticancer activity against five different human tumor cell lines including prostate (PC3), lung (A549), brain (U87MG), and breast (MCF7 and MDA-MB-231) using MTT assay and the results are illustrated in Table.1. The results from Table 1 indicated that most of the synthesised compounds (**7**, **9a-j**) except **9k** displayed moderate to potent growth inhibition against the tested cancer cells and selective potency against MDA-MB-231 cells. Compounds **9a**, **9c-9d** and **9f-9i** displayed remarkable growth inhibition on MDA-MB-231 cells which are superior to the standard 5-Fluorouracil. Moreover, **9a**, **9c** and **9f** displayed significant broad spectrum growth inhibition against all the tested cancer cells with IC₅₀ values in the range of 0.71-8.23 μ M. Further, **9c** displayed selective potency growth inhibition of PC-3 (IC₅₀-0.47 μ M) and MCF-7 (IC₅₀-0.65 μ M) cell lines which are superior to the standard drug 5-Fluorouracil. Interestingly, *N*-propargylated compound **7** that doesn't contain triazole ring also exhibited considerable anti-tumour activity against PC-3 tumour cells (IC₅₀- 0.98 μ M) and breast cancer cells MCF-7 (IC₅₀-7.63 μ M). Substituents at *meta*-position of the ring **C** seemed to have significant effect on activity for example, as both 3-NO₂ (**9c**) and 3-F (**9f**) substituted compounds exhibited significant growth inhibition activities. However, the unsubstituted compound (**9a**) on the **C** ring also displayed substantial growth inhibition. On the other hand, *para*-substituted compounds displayed mixed results. For instance, 4-fluoro (**9d**), 4-trifluoromethoxy (**9k**), and 4-nitro (**9b**) substituted compounds are ineffective and 4-chloro (**9g**) scaffold showed remarkable cytotoxic activity.

<Table 1>

2.2.2 Colony formation inhibition assay

Anti-proliferative activity of the most active compound in the series **9a** was further confirmed by clonogenic cell survival assay on A549 and MDA-MB-231 cells. This assay reflects the capability of a single cell to rise into a colony and it is also considered as the standard for determining long term cell viability because they reflect all modes of cell death or arrest [28]. As shown in Figure 3 treatment of A549 and MDA-MB-231 cells with **9a** resulted in inhibition of colony formation in a dose dependent manner. The formation of colonies was completely inhibited by the compound **9a** at 10 μ M concentration in both the treated cells. This indicates the ability of **9a** on dose dependent inhibition of colony formation ability and proliferation of A549 and MDA-MB-231 cells.

<Figure 3>

2.2.3 *In vitro* cell migration assay

Migratory and invasive activities of tumor cells are the important characteristics of metastatic cancers. Therefore, it was of interest to investigate the effect of compound **9a** on tumor cell migration using wound healing assay [29]. Artificial wounds were created in the confluent monolayer A549 and MDA-MB-231 cells using sterile 200 μ L pipette tip and were treated with the different concentrations of compound **9a**. Images were taken immediately (0 h) and 24 and 48 h after treatment. As depicted in Figure 4 treatment with **9a** resulted in suppression of A549 and MDA-MB-231 cell migration to the wounded area in a concentration dependent manner in comparison to the control.

<Figure 4>

2.2.4 Cell cycle analysis

We next analysed the effect of compound **9a** on cell cycle distribution using flow cytometry. A549 and MDA-MB-231 tumor cells were treated with different concentrations (0.5, 1 and 2 μ M) of **9a** for 48 h; cells were fixed in ethanol and stained with propidium iodide. Results from the Figure 5 revealed that the proportion of A549 and MDA-MB-231 cells in G2/M phase gradually increased respectively from 31% (control) to 51% (2 μ M) and 20% (control) to 63 % (2 μ M). Similarly, the population in G0/G1 phase declined from 49% to 34% and 73% to 33%, respectively after treatment with the compound. This indicates that **9a** treatment resulted in the arrest of A549 and MDA-MB-231 cells in G2/M phase of cell cycle.

<Figure 5>

2.2.5 Apoptosis detection studies

Apoptosis is a programmed cell death which plays an important role in the maintenance of tissue homeostasis and cell survival. Disruption or inappropriate regulation of apoptotic processes results in several diseases including cancer [30]. Thus, inducing apoptosis in cancer cells has emerged as an attractive strategy in cancer therapy [31].

2.2.5.1 Hoechst staining

Chromatin condensation, nuclear shrinking and DNA fragmentation are the typical characteristics of an apoptotic cell. Therefore, apoptosis inducing effect of compound **9a** was investigated using the Hoechst staining (H 33242) assay. A549 and MDA-MB-231 cells treated with different concentrations of **9a** for 48 h were stained with Hoechst. As evident from Figure 6, control, A549 and MDA-MB-231 cells treated with DMSO showed uniformly dispersed chromatin, whereas compound **9a** treated cells displayed typical apoptotic characteristics such as condensation of nuclei (arrowheads indicates apoptotic nuclei). These findings demonstrate that **9a** could induce apoptosis in A549 and MDA-MB-231 cells.

<Figure 6>

2.2.5.2 Effect of compounds on mitochondrial membrane potential ($\Delta\Psi_m$)

Mitochondrial membrane potential regulates the mitochondrial permeability and plays an important role in triggering apoptosis [32]. In order to further investigate the apoptosis-inducing effect of compound **9a**, changes in the mitochondrial membrane potential were measured using rhodamine-123 staining. Mitochondria with the intact $\Delta\Psi_m$ can hold the Rh-123 probe and exhibits strong green fluorescence. Loss of $\Delta\Psi_m$ results in decrease in green fluorescence due to the lack of Rhodamine-123 retention [33]. A549 and MDA-MB-231 cells were treated with **9a** for 48 h, and then stained with Rhodamine-123. The results from Figure 7 indicated that, treatment of **9a** induced 20-35% decrease in $\Delta\Psi_m$ in MDA-MB-231 cancer cells and 15-30% in A549 cells in concentration dependant manner in compared to respective control cells, which indicates that **9a** induces apoptosis in A549 and MDA-MB-231 cells through change in $\Delta\Psi_m$.

<Figure 7>

2.2.5.3 Measurement of reactive oxygen species (ROS) levels

Decline in mitochondrial membrane potential ($\Delta\Psi_m$) and increase in the level of intracellular ROS are closely related in the course of apoptosis. Moreover, generation of ROS is considered as one of the key mediators of apoptotic signalling and many if not most of the anti-tumour agents exhibit their cytotoxic effects through the generation of ROS [34, 35]. Thus to investigate whether ROS accumulation was involved in compound **9a** induced apoptosis, A549 and MDA-MB-231 cells were treated with different concentrations of compound **9a** for 48 h and incubated with carboxy-DCFDA to inspect **9a** mediated production of ROS. As shown in Figure 8, there is a gradual increase in green carboxy-DCF fluorescence (correlates with ROS concentration) with increasing the concentration of compound **9a** treated A549 (1.8-2.5 times) and MDA-MB-231 (2.09-2.98 times) (Figure 8) cells and it is

more prominent with MDA-MB-231 cells. These results clearly indicate that **9a** could induce the ROS generation.

<Figure 8>

2.2.5.4 Annexin V-FITC/Propidium iodide dual staining assay

To quantify the percentage of apoptosis induced by the compound **9a**, Annexin V-FITC-PI dual staining assay has been carried out which facilitates the detection of live cells (Q1-LL; AV-/PI-), early apoptotic cells (Q1-LR; AV+/PI-), late apoptotic cells (Q1-UR-AV+/PI+) and necrotic cells (Q1-UL; AV-/PI+). As shown in Figure 9, the percentage of total apoptotic cells (early and late apoptotic cells) was increased to 32.4 % (MDA-MB-231) and 34.9% (A549) after treatment with compound **9a** (2 μ M), in comparison to the control MDA-MB-231 (9.8%) and A549 (6.5%) cells respectively. The percentage of early and late apoptotic cells were markedly increased with increase in concentration of the compound **9a**. Therefore, these results confirmed that the compound **9a** treated MDAMB-231 and A549 cells undergo apoptosis in a dose dependent manner.

<Figure 9>

3.0 Conclusion

In an effort to discover novel anti-cancer agents, a series (**9a-k**) of dibenzodiazepinone-triazole derivatives were prepared, characterized and evaluated against five human tumour cell lines. All the synthesized compounds exhibited moderate to good activity against five cancer cell lines. In particular, compound **9a** exhibited potent *in vitro* anti-cancer activity among the tested compounds with the IC₅₀ values in the range of 0.71 to 7.29 μ M. It is evident from the cell migration and clonogenic experiments that, migration and colony formation of the A549 and MDA-MB-231 cells was significantly affected by compound **9a**. Flow cytometry analysis revealed that **9a** arrested both these cells in G2/M phase. Further

apoptosis studies conducted on A549 and MDA-MB-231 cells revealed that compound **9a** effectively induces apoptosis through drop in mitochondrial membrane potential ($\Delta\Psi_m$) and increases the ROS generation in A549 and MDA-MB-231. Overall, these results suggest that compound **9a** has the potential to be developed as lead and their further structural modification may produce promising anticancer agents.

4.0 Experimental section

4.1 Chemistry

All reagents and solvents were of commercial grade purchased and used without further purification. Melting points were recorded after column chromatography of compound on Electro thermal melting point apparatus and were uncorrected. ^1H NMR, ^{19}F NMR (300 MHz) and ^{13}C NMR (75 MHz) spectra were recorded in CDCl_3 or CD_3SOCD_3 solvents on Bruker Avance 300 MHz spectrometer at ambient temperature. Chemical shifts (δ) are reported in ppm downfield from internal TMS standard. Signal multiplicities are represented by s (singlet), d (doublet), t (triplet), dd (double doublet), m (multiplet) and br s (broad singlet). HRMS results were run on the AB Sciex QSTAR ELITE mass spectrometer using an electron spray ionization ESI source. IR spectra were recorded on Perkin-Elmer Infrared spectrometer and samples were scanned in grounded KBr powder. Routine monitoring of reaction was performed by TLC (Thin layer chromatography) on aluminium silica plates obtained from E-Merck. For TLC visualisation UV light and iodine were used. All the column chromatographic separations were done by using silica gel (Acme's, 60-120 mesh). Evaporation of solvents was performed at reduced pressure on a rotary evaporator.

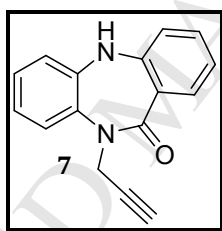
4.1.1 5,10-Dihydro-11H-dibenzo[b,e][1,4]diazepin-11-one (1)

To a dried pressure tube was added *o*-phenylenediamine (0.3 g, 2.7 mmol), ethyl-2-iodobenzoate (1.5 g, 5.5 mmol) under nitrogen followed by ethylene glycol (6 mL), 10 mol % CuI (52 mg, 0.27 mmol) and K_3PO_4 tribasic (1.17 g, 5.5 mmol). Pressure tube was closed

tightly and heated at 100 °C for 4 h. After completion of the reaction (monitored by TLC) reaction mixture was cooled to room temperature and filtered over a pad of silica with CH₂Cl₂ to remove CuI and base residues. Then solvent was removed on rotary evaporator and the residue was purified on silica column chromatography using 25-30% EtOAc in hexane as solvent to give **1** Yield 50% (0.29 g)

mp: 251-253 °C; IR (ν_{\max}): 3320, 3025, 1603, 1579, 1471, 1394, 1157, 748 cm⁻¹; ¹H NMR (300 MHz, DMSO-*d*₆): δ 8.63 (s, 1H, Amide NH), 6.60 (s, 1H, Amine NH), 6.46 (dd, *J* = 7.9, 1.4 Hz, 1H, ArH), 6.19 – 6.08 (m, 1H, ArH), 5.87 – 5.63 (m, 6H, ArH); ¹³CNMR (75 MHz, DMSO): δ 168.1, 150.4, 140.0, 133.2, 131.9, 129.6, 124.6, 123.0, 122.7, 121.2, 120.9, 119.8, 119.0 ;HRMS (ESI) *m/z* calculated for [M+H]⁺ [C₁₃H₁₁N₂O] 211.0866, found 211.0860.

4.1.2 10-(Prop-2-yn-1-yl)-5,10-dihydro-11H-dibenzo[*b,e*][1,4]diazepin-11-one (7)



In a two neck round bottom flask compound **2** (0.1 g, 0.47 mmol) was dissolved in freshly distilled dry THF (5 mL), under inert conditions. To that was added 1.5 mL of 1.6 M *n*-BuLi (5 equiv) at -20 °C. After 5 min 80% propargyl bromide in toluene (0.054 mL, 0.52 mmol) was added to the reaction and the mixture stirred for 1 h at the same temperature. Reaction was monitored by TLC after consumption of the starting material reaction was quenched with saturated NH₄Cl solution and partitioned between H₂O and EtOAc. Organic layers were separated, combined, dried over anhydrous Na₂SO₄ and concentrated on rotary evaporator below 46 °C. Product was purified on silica column chromatography to yield propargylated scaffold **7**.

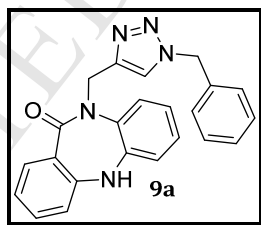
Yield: 72 % (80 mg); mp: 165-170 °C ; IR (ν_{\max}): 3321, 3292, 2923, 1623, 1546, 1454, 1160 cm⁻¹; ¹H NMR (300 MHz, CDCl₃): δ 7.94 (dd, *J* = 7.8, 1.3 Hz, 1H, ArH), 7.72 – 7.57 (m, 1H,

ArH), 7.39 – 7.25 (m, 1H, ArH), 7.20 – 6.90 (m, 4H, ArH), 6.83 (d, $J = 8.0$ Hz, 1H, ArH), 5.53 (s, 1H, NH), 4.68 (d, $J = 2.4$ Hz, 2H, propargylic-CH₂), 2.39 (t, $J = 2.4$ Hz, 1H, triple bond H); ¹³CNMR (75 MHz, CDCl₃): δ 168.1, 150.6, 143.1, 134.3, 133.1, 132.8, 126.2, 124.4, 124.2, 122.9, 122.6, 120.3, 118.6, 80.1, 72.0, 40.3 ; HRMS (ESI): m/z calculated for [M+H]⁺ [C₁₆H₁₃N₂O] is 249.1022 found 249.1015

4.1.3 General procedure for the click reaction:

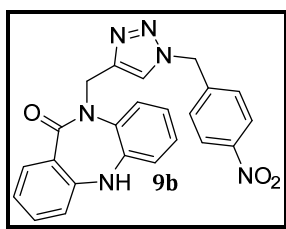
To the propargylated compound **7** (50 mg, 0.20 mmol) and azide **8a-k** (0.60 mmol) in 3 mL of 1:1 *t*-BuOH/H₂O was added 100 μ L saturated CuSO₄·5H₂O solution followed by catalytic amount of Na-ascorbate at ambient temperature. Reaction was allowed to stir for 5-6 h, solvent was removed and product was extracted with CH₂Cl₂. Dichloromethane layer was dried over anhydrous sodium sulphate, solvent was evaporated *in vacuo* and residue was purified using silica column chromatography to obtain **9a-k**.

4.1.3.1 10-((1-Benzyl-1H-1,2,3-triazol-4-yl)methyl)-5,10-dihydro-11H-dibenzo[*b,e*][1,4]diazepin-11-one (**9a**)



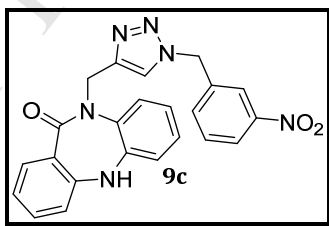
Yield: 82% (50 mg); mp: 128-133 °C; IR (ν_{\max}): 3301, 3069, 2936, 2123, 1631, 1480, 1320, 1160, 765 cm⁻¹; ¹H NMR (300 MHz, CDCl₃) δ : 7.77 – 7.65 (m, 2H), 7.61 (dd, $J = 7.5, 1.6$ Hz, 1H, ArH), 7.35 – 7.10 (m, 6H, ArH), 7.05 – 6.85 (m, 3H, ArH), 6.80 (dd, $J = 7.4, 3.8$ Hz, 1H, ArH), 6.71 (d, $J = 7.9$ Hz, 1H, ArH), 5.42 (s, 3H, benzyl-CH₂&-NH), 5.13 (d, $J = 12.5$ Hz, 2H, triazole-CH₂); ¹³CNMR (75 MHz, CDCl₃) δ : 168.6, 150.8, 143.4, 134.7, 134.7, 132.6, 129.0, 128.6, 127.9, 126.1, 125.0, 124.6, 124.2, 122.6, 120.2, 118.6, 54.1, 47.1; HRMS (ESI): m/z calculated for [M+H]⁺ [C₂₃H₂₀N₅O] 382.1662 found 382.1663.

4.1.3.2 10-((1-(4-Nitrobenzyl)-1H-1,2,3-triazol-4-yl)methyl)-5,10-dihydro-11H-dibenzo[*b,e*][1,4]diazepin-11-one (9b)



Yield: 61% (31 mg); mp: 159-164 °C; IR (ν_{\max}): 3132, 3075, 1628, 1522, 1474, 1344, 1049, 767 cm^{-1} ; ^1H NMR (300 MHz, CDCl_3) δ : 8.13 (d, $J = 8.7$ Hz, 2H, ArH), 7.79 (s, 1H, triazole H), 7.68 (d, $J = 8.1$ Hz, 1H, ArH), 7.60 (d, $J = 7.6$ Hz, 1H), 7.32-7.16 (m, 3H, ArH), 7.06-6.88 (m, 3H, ArH), 6.81 (d, $J = 7.5$ Hz, 1H, ArH), 6.72 (d, $J = 8.0$ Hz, 1H, ArH), 5.54 (s, 2H, benzylic- CH_2), 5.33 (brs, 1H, -NH), 5.13 (s, 2H, triazole- CH_2); ^{13}C NMR (75 MHz, CDCl_3) δ : 168.7, 150.7, 148.0, 145.9, 143.3, 141.7, 134.7, 132.7, 132.5, 128.5, 126.2, 124.9, 124.8, 124.7, 124.2, 124.1, 122.7, 120.2, 118.6, 53.0, 47.1; HRMS (ESI): m/z calculated for $[\text{M}+\text{H}]^+$ [$\text{C}_{23}\text{H}_{19}\text{N}_6\text{O}_3$] 427.1513, found 427.1504.

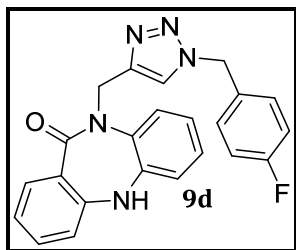
4.1.3.3 10-((1-(3-Nitrobenzyl)-1H-1,2,3-triazol-4-yl)methyl)-5,10-dihydro-11H-dibenzo[*b,e*][1,4]diazepin-11-one (9c)



Yield: 68 % (35 mg); mp: 124-130 °C; IR (ν_{\max}): 3314, 3012, 2102, 1634, 1528, 1477, 1350, 758 cm^{-1} ; ^1H NMR (300 MHz, CDCl_3) δ : 8.26-8.17 (m, 1H), 8.14 (s, 1H), 7.89 (s, 1H), 7.80 (dd, $J = 12.2, 8.2$ Hz, 1H, ArH), 7.67 (d, $J = 8.8$ Hz, 1H, ArH), 7.62 – 7.52 (m, 2H, ArH), 7.31 (m, 1H, ArH), 7.14-6.86 (m, 4H, ArH), 6.81 (d, $J = 7.9$ Hz, 1H, ArH), 5.63 (s, 2H, benzylic- CH_2), 5.45 (s, 1H, -NH), 5.24 (s, 2H, triazole- CH_2); ^{13}C NMR (75 MHz, CDCl_3) δ : 168.7, 150.7, 143.4, 136.8, 134.6, 133.8, 132.7, 132.5, 130.2, 126.2, 124.9, 124.7, 124.1,

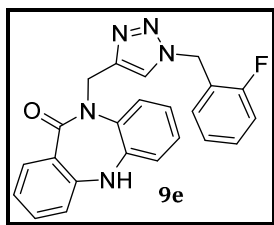
123.6, 122.8, 122.7, 120.3, 118.6, 53.1, 47.0; HRMS (ESI): m/z calculated for $[M+H]^+$ $[C_{23}H_{19}N_6O_3]$ 427.1513, found 427.1503.

4.1.3.4 10-((1-(4-Fluorobenzyl)-1H-1,2,3-triazol-4-yl)methyl)-5,10-dihydro-11H-dibenzo[*b,e*][1,4]diazepin-11-one (9d)



Yield: 70% (43 mg); mp: 109-114 °C; IR (ν_{max}): 3305, 3129, 3069, 1628, 1513, 1474, 1154, 764 cm^{-1} ; 1H NMR (300 MHz, $CDCl_3$) δ : 7.70 (s, 1H, triazole H), 7.68 (dd, $J = 1.6, 7.8$ Hz, 1H, ArH), 7.62 (dd, $J = 1.8, 7.8$ Hz, 1H, ArH), 7.25-7.12 (m, 3H, ArH), 7.05-6.89 (m, 5H, ArH), 6.80 (dd, $J = 1.9, 7.4$ Hz, 1H, ArH), 6.72 (d, $J = 7.9$ Hz, 1H, ArH) 5.40 (s, 2H, benzylic- CH_2), 5.31 (brs, 1H, NH), 5.10 (s, 2H, triazole- CH_2); ^{13}C NMR (75 MHz, $CDCl_3$) δ : 168.6, 150.7, 145.6, 143.3, 134.7, 132.6, 132.6, 130.6, 130.5, 129.9, 129.8, 126.1, 124.9, 124.7, 124.4, 124.2, 122.7, 120.1, 118.5, 116.2, 115.9, 53.3, 47.1; ^{19}F NMR (300 MHz, $CDCl_3$) δ : -112.7-112.9 (m); HRMS (ESI): m/z calculated for $[M+H]^+$ $[C_{23}H_{19}FN_5O]$ 400.1568 found 400.1567.

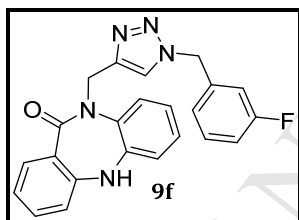
4.1.3.5 10-((1-(2-Fluorobenzyl)-1H-1,2,3-triazol-4-yl)methyl)-5,10-dihydro-11H-dibenzo[*b,e*][1,4]diazepin-11-one (9e)



Yield: 73 % (35 mg); mp: 168-173 °C; IR (ν_{max}): 3326, 3151, 3057, 1613, 1486, 1226, 1042, 758 cm^{-1} ; 1H NMR (300 MHz, $CDCl_3$) δ : 7.87 (s, 1H, triazole H), 7.80 (dd, $J = 7.8, 1.3$ Hz, 1H, ArH), 7.70 (dd, $J = 7.4, 1.6$ Hz, 1H, ArH), 7.46-6.97 (m, 8H, ArH), 6.90 (d, $J = 7.3$ Hz,

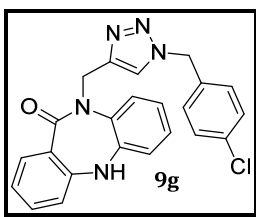
1H, ArH), 6.82 (d, $J = 7.9$ Hz, 1H, ArH), 5.59 (s, 2H, benzylic-CH₂), 5.45 (s, 1H, -NH), 5.22 (s, 2H, triazole-CH₂); ¹³CNMR (75 MHz, CDCl₃) δ : 168.6, 162.1, 158.8, 150.7, 143.3, 134.7, 132.6 (split), 130.8 (split), 130.7, 130.3, 126.1, 125.0, 124.7, 124.2 (split), 122.7, 122.0, 121.9, 120.2, 118.5, 115.9, 115.6, 47.6 (split), 47.1; ¹⁹F NMR (300 MHz, CDCl₃) δ -117.8-118.0 (m); HRMS (ESI): m/z calculated for [M+H]⁺ [C₂₃H₁₉FN₅O] 400.1568 found 400.1563.

4.1.3.6 10-((1-(3-Fluorobenzyl)-1H-1,2,3-triazol-4-yl)methyl)-5,10-dihydro-11H-dibenzo[*b,e*][1,4]diazepin-11-one (9f)



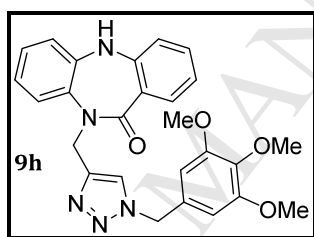
Yield: 70% (33 mg); mp: 143-148 °C ; IR (ν_{\max}): 3312, 3051, 1622, 1471, 1120, 766 cm⁻¹; ¹H NMR (300 MHz, CDCl₃) δ : 7.73 (s, 1H, triazole H), 7.69 (dd, $J = 7.8, 1.4$ Hz, 1H, ArH), 7.60 (dd, $J = 7.6, 1.7$ Hz, 1H, ArH), 7.31-7.15 (m, 3H, ArH), 7.07-6.87 (m, 6H, ArH), 6.81 (dd, $J = 12.6, 5.3$ Hz, 2H, ArH), 6.72 (d, $J = 7.9$ Hz, 1H, ArH), 5.42 (s, 2H), 5.14 (s, 2H, triazole-CH₂); ¹³CNMR (75 MHz, CDCl₃) δ : 168.6, 164.6, 161.3, 150.7, 143.4, 137.0, 134.6, 132.6, 130.7, 130.6, 126.2, 124.9, 124.7, 124.2, 123.5, 122.7, 120.2, 118.6, 115.8, 115.5, 115.0, 114.7, 53.5, 47.0; ¹⁹F NMR (300 MHz, CDCl₃) δ : -111.6 (td, $J = 8.9, 5.9$ Hz); HRMS (ESI): m/z calculated for [M+H]⁺ [C₂₃H₁₉FN₅O] 400.1568 found 400.1569.

4.1.3.7 10-((1-(4-Chlorobenzyl)-1H-1,2,3-triazol-4-yl)methyl)-5,10-dihydro-11H-dibenzo[*b,e*][1,4]diazepin-11-one (9g)



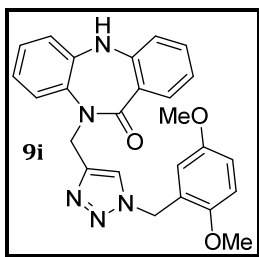
Yield: 75% (50 mg); mp: 135-140 °C; IR (ν_{\max}): 3307, 3135, 1624, 1479, 1395, 1157, 1052, 766 cm^{-1} ; ^1H NMR (300 MHz, CDCl_3) δ : 7.71 (s, 1H, triazole H), 7.68 (dd, $J = 1.7, 8.0$ Hz, 1H, ArH), 7.60 (dd, $J = 2.0, 7.4$ Hz, 1H, ArH), 7.28-7.16 (m, 4H, ArH), 7.12-7.06 (m, 2H, ArH), 7.04-6.88 (m, 3H, ArH), 6.79 (dd, $J = 1.8, 7.1$ Hz, 1H, ArH), 6.71 (d, $J = 7.9$ Hz, 1H, ArH) 5.39 (s, 2H, benzylic- CH_2), 5.34 (brs, 1H, NH), 5.11 (s, 2H, triazole- CH_2); ^{13}C NMR (75 MHz, CDCl_3) δ : 168.6, 150.7, 145.6, 143.3, 134.7, 134.6, 133.2, 132.6, 132.6, 129.3, 129.2, 126.1, 124.9, 124.7, 124.5, 124.1, 122.7, 120.2, 118.5, 53.6, 47.2; HRMS (ESI): m/z calculated for $[\text{M}+\text{H}]^+$ [$\text{C}_{23}\text{H}_{19}\text{ClN}_5\text{O}$] 416.1273, found 416.1236.

4.1.3.8 10-((1-(3,4,5-Trimethoxybenzyl)-1H-1,2,3-triazol-4-yl)methyl)-5,10-dihydro-11H-dibenzo[*b,e*][1,4]diazepin-11-one (9h)



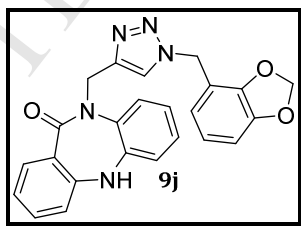
Yield: 90% (80 mg); mp: 122-128 °C; IR (ν_{\max}): 3311, 3132, 3946, 1631, 1504, 1462, 1238, 1126, 761 cm^{-1} ; ^1H NMR (300 MHz, CDCl_3) δ : 7.76 (s, 1H, triazole H), 7.68 (dd, $J = 7.8, 1.4$ Hz, 1H, ArH), 7.61 (dd, $J = 7.5, 1.7$ Hz, 1H, ArH), 7.27-7.17 (m, 2H, ArH), 7.06-6.89 (m, 3H, ArH), 6.85-6.76 (m, 1H, ArH), 6.73 (d, $J = 7.9$ Hz, 1H, ArH), 6.41 (s, 2H, ArH), 5.36 (s, 2H, benzylic- CH_2), 5.14 (s, 2H, triazole- CH_2), 3.79 – 3.72 (m, 9H, $-\text{OCH}_3$); ^{13}C NMR (75 MHz, CDCl_3) δ : 168.6, 153.6, 150.7, 143.3, 138.2, 134.7, 132.7, 132.5, 130.1, 126.2, 124.9, 124.7, 124.6, 124.1, 122.7, 120.2, 118.6, 105.2, 60.8, 56.2, 54.5, 47.1; HRMS (ESI): m/z calculated for $[\text{M}+\text{H}]^+$ [$\text{C}_{26}\text{H}_{26}\text{O}_4\text{N}_5$] 472.1979 found 472.1961.

4.1.3.9 10-((1-(2,5-Dimethoxybenzyl)-1H-1,2,3-triazol-4-yl)methyl)-5,10-dihydro-11H-dibenzo[*b,e*][1,4]diazepin-11-one (9i)



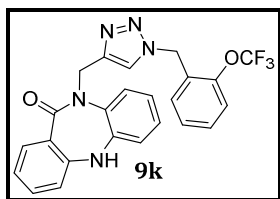
Yield: 68% (50 mg); mp: 111-115 °C; IR (ν_{\max}): 3259, 3220, 2948, 1640, 1504, 1226, 1036, 770 cm^{-1} ; ^1H NMR (300 MHz, CDCl_3) δ : 7.84 (s, 1H, triazole H), 7.76 (ddd, $J = 1.6, 7.7, 13.9$ Hz, 2H, ArH), 7.34-7.27 (m, 1H, ArH), 7.14-6.97 (m, 3H, ArH), 6.92-6.83 (m, 3H, ArH), 6.80 (d, $J = 7.9$ Hz, 1H, ArH), 6.72 (d, $J = 7.6$ Hz, 1H, ArH), 6.75-6.71 (m, 1H, ArH), 5.51 (s, 2H, benzylic- CH_2), 5.37 (brs, 1H, NH), 5.20 (s, 2H, triazole- CH_2), 3.83 (s, 3H, $-\text{OCH}_3$), 3.74 (s, 3H, $-\text{OCH}_3$); ^{13}C NMR (75 MHz, CDCl_3) δ : 168.5, 153.6, 151.2, 150.7, 144.9, 143.3, 134.8, 132.6, 132.5, 126.0, 125.1, 124.8, 124.7, 124.3, 124.0, 122.6, 120.1, 118.5, 115.8, 114.7, 111.7, 55.9, 55.7, 49.0, 47.1; HRMS (ESI): m/z calculated for $[\text{M}+\text{H}]^+$ [$\text{C}_{25}\text{H}_{24}\text{O}_3\text{N}_5$] 442.1874 found 442.1876.

4.1.3.10 10-((1-(Benzo[d][1,3]dioxol-4-ylmethyl)-1H-1,2,3-triazol-4-yl)methyl)-5,10-dihydro-11H-dibenzo[b,e][1,4]diazepin-11-one (9j)



Yield: 80% (41 mg); mp: 118-123 °C; IR (ν_{\max}): 3328, 2922, 1670, 1451, 1035, 772 cm^{-1} ; ^1H NMR (300 MHz, CDCl_3) δ : 7.86-7.75 (m, 2H, ArH & triazole-H), 7.71 (d, $J = 7.5$ Hz, 1H, ArH), 7.36-7.24 (m, 1H, ArH), 7.17- 6.97 (m, 3H, ArH), 6.94-6.70 (m, 5H, ArH), 5.99 (s, 2H, $-\text{O}-\text{CH}_2-\text{O}-$), 5.42 (s, 2H, benzylic- CH_2), 5.38 (brs, 1H, $-\text{NH}$), 5.20 (s, 2H, triazole- CH_2); ^{13}C NMR (75 MHz, CDCl_3) δ : 168.6, 150.7, 148.2, 147.9, 145.4, 143.3, 134.7, 132.6, 132.6, 128.3, 126.1, 125.0, 124.7, 124.2, 122.7, 121.9, 120.1, 118.5, 108.5, 108.5, 101.3, 54.0, 47.1; HRMS (ESI): m/z calculated for $[\text{M}+\text{H}]^+$ [$\text{C}_{24}\text{H}_{20}\text{O}_3\text{N}_5$] 426.1566 found 426.1563.

4.1.3.11 10-((1-(2-(Trifluoromethoxy)benzyl)-1H-1,2,3-triazol-4-yl)methyl)-5,10-dihydro-11H-dibenzo[*b,e*][1,4]diazepin-11-one (9k)



Yield: 80% (45 mg); mp:130-135 °C; IR (ν_{\max}): 3305, 2927, 2958, 1628, 1477, 1253, 1048, 761 cm^{-1} ; ^1H NMR (300 MHz, CDCl_3) δ 7.76 (s, 1H, triazole-H), 7.71 (dd, $J = 7.8, 1.4$ Hz, 1H, ArH), 7.66-7.56 (m, 1H, ArH), 7.33 (m, 1H, ArH), 7.29-7.16 (m, 4H), 7.13-6.90 (m, 4H, ArH), 6.85-6.77 (m, 1H, ArH), 6.72 (d, $J = 7.9$ Hz, 1H, ArH), 5.55 (s, 2H, benzylic- CH_2), 5.28 (s, 1H, -NH), 5.15 (s, 2H, triazole- CH_2); ^{13}C NMR (75 MHz, CDCl_3) δ :168.5, 150.6, 146.8, 143.3, 134.7, 132.6, 130.2, 130.1, 127.4, 126.1, 125.0, 124.7, 124.2, 122.7, 120.5, 120.1, 118.5, 48.4, 47.0; ^{19}F NMR (300 MHz, CDCl_3) δ -57.21 (d, $J = 1.5$ Hz); HRMS (ESI): m/z calculated for $[\text{M}+\text{H}]^+$ [$\text{C}_{24}\text{H}_{19}\text{F}_3\text{N}_5\text{O}_2$] 466.1491 found 466.1504.

4.3 Biology

4.3.1 Cell culture

PC-3, A549, U87MG, MCF-7 and MDA-MB-231 cells were purchased from ATCC (Manassas, VA). The PC-3, A549 and MDA-MB-231 cells were grown in RPMI 1640 medium (GIBCO-Invitrogen, NY) with 10% fetal bovine serum (FBS) and supplemented with penicillin G (100 $\mu\text{g}/\text{mL}$), glutamine (2 mmol/L), and streptomycin (100 $\mu\text{g}/\text{mL}$) at 37 °C under 5% CO_2 . U87MG and MCF-7 cells were cultured in Dulbecco's modified Eagle's medium (DMEM) containing 10% fetal bovine serum (FBS), 1% penicillin/ streptomycin at 37 °C under 5% CO_2 . The medium was changed every two days. After reaching 80-90% confluence, cells were treated with 0.25% trypsin-EDTA for further passage. For all the experiments cells were used at passages 4-10.

4.3.2 MTT assay

MTT cell proliferation assay was conducted on PC-3, A549, U87MG, MCF-7 and MDA-MB-231 cancer cell lines to test the compounds **9a-k**, **1** and **7**. Cells were seeded at a density of 3000-5000 cells per well in a 96 well plate depending on the doubling time. Seeded plates were allowed for 24 h at 37 °C and 5% CO₂ in incubator. After 24 h, the culture media was removed; 100µL of test compounds dissolved in DMSO and culture media was added to the cells in each well. Wells in which test compound was not added (containing only culture medium and DMSO) were used as the control. Then, the compound treated cells were incubated for 72 h maintaining the same conditions. 72 h later, culture medium was removed and 100 µL of MTT (Thiazoyl blue tetrazolium bromide) solution (5 mg/mL in culture media) was added to each well including control wells and further incubated for 4 h. When the purple precipitate was visible in wells, media containing MTT was aspirated from the wells and to each well 100 µL of DMSO was added to dissolve the Formazan product. Plate covers were removed and absorbance in each well was measured in microtiter plate reader at 570 nm and a reference wavelength of 630 nm. The absorbance readings at 630 nm were subtracted from the 570 nm readings and the results were adjusted by dividing the average by the DMSO control to adjust for any toxicity that may have occurred in this control treatment set. The percentage inhibition was calculated as $100 - [(Mean\ OD\ of\ treated\ cell \times 100) / Mean\ OD\ of\ vehicle\ treated\ cells\ (DMSO)]$. The IC₅₀ Values were calculated using Probit Software. All the tests were repeated in at least three independent experiments.

4.3.3 Colony formation inhibition assay

A549 and MDA-MB-231 cells at the exponential phase were plated at a single cell density (500 cells/well) in two separate 6 well plates and allowed to adhere for 24 h in the incubator. Then, cells were incubated with culture medium containing compound **9a** in 10, 1 and 0.1 µM concentrations. After 24 h, the medium was replaced with fresh culture medium and cells

were incubated for further 14 days. The cells were washed with PBS, fixed with 4 % para formaldehyde and stained with 0.5% methylene blue in PBS for 30 min. Then, excess dye was rinsed off with distilled water several times. Plates were photographed with a digital camera.

4.3.4 Cell cycle analysis

A549 and MDA-MB-231 cells were seeded in 6 well plates at a density of 1×10^6 cells/well and after 24 h; cells were treated with compound **9a** in three different concentrations 0.5, 1 and $2 \mu\text{M}$. Cells treated with DMSO were used as control. 48 h after treatment, both floating and trypsinised cells were harvested and washed with PBS. Cells were fixed with 70% ethanol for 30 mins at 4°C . Then, cells were centrifuged (1200 rpm for 5 min), the supernatant was discarded and the pellet was washed with PBS and stained the cells with propidium iodide staining buffer (PI (200 μg), 0.1% (v/v) Triton X-100, 2 mg DNase-free RNase A (Sigma) in 10 mL PBS)) for 15 min at ambient temperature in absence of light. Later, samples were analysed for propidium iodide-DNA fluorescence from 10000 events by flow cytometry using BD-C6 accuri flow cytometer.

4.3.5 *In vitro* Migration Assay

The wound healing assay has been used to examine the cell migration. In two separate 6 well plates A549 cells and MDA-MB-231 cells (5×10^5 cells per well) were cultured as confluent monolayers for 24 h. Then, using 200 μL sterile pipette tip the monolayers were gently scraped one time in the middle from one end to the other end to create a denuded zone of constant width. The wounded mono layers were twice washed with phosphate saline buffer (PBS) to remove non-adherent cells. Then, cells were treated with compound **9a** in different concentrations (0.5, 1 and $2 \mu\text{M}$). Cell migration across the inflicted wounds were photographed under the phase contrast microscope (Nikon) in 0 , 24 and 48 h time intervals in three or more randomly selected fields.

4.3.6 Hoechst staining

A549/MDA-MB-231 cells (25×10^4 cells/well) at their growth phase were seeded and allowed for 24 h to adhere. Test compound **9a** in three different concentrations 0.5, 1 and $2 \mu\text{M}$ in culture medium was added to the cells and incubated for 48 h at 37°C . Then, culture medium was removed from the wells, washed with PBS and stained with Hoechst 33242 ($5 \mu\text{g/mL}$) for half an hour at room temperature. Excess dye was removed by PBS washing twice after which, morphological changes in the cells were examined with fluorescence microscope using 350 nm excitation and 460 nm emission (Nikon, magnification 10X).

4.3.7 Measurement of Mitochondrial membrane Potential (MMP)

In a 6 well plate A549/MDA-MB-231MDA-MB-231 cells were cultured at a density of 5×10^5 cells/mL and incubated for overnight. Then the test compound at 0.5, 1 and $2 \mu\text{M}$ concentrations was added to the wells. 24 h after the treatment, adherent cells were collected by trypsinisation, washed with PBS ($500 \mu\text{L}$) and treated with the $400 \mu\text{L/well}$ of Rhodamine-123 solution in PBS ($2 \mu\text{M}$) in the absence of light. After 30 min of incubation at room temperature, cells were twice washed with PBS and resuspended in PBS. The samples were then analysed for fluorescence using spectrofluorometer.

4.3.8 Measurement of reactive Oxygen Species (ROS) levels

A549 cells were seeded in a 6 well plate at a density of 5×10^5 cells/mL and allowed to grow overnight. The cells were incubated with the 0.5, 1 and $2 \mu\text{M}$ concentration of compound **9a** for 24 h. After which the medium was removed from the wells, culture medium containing DCFDA ($10 \mu\text{M}$) was added to the wells in the dark and incubated for half an hour at ambient temperature. Cells were washed with PBS, collected and resuspended in PBS. Intensity of the formed 2', 7'-dichlorofluorescein as a result of Carboxy-DCFDA hydrolysis, was analysed in spectrofluorometer at an excitation and emission wavelength of 488 and 525 nm respectively.

Qualitative cellular fluorescence images were captured by Nikon ECLIPSETE2000-S fluorescence microscope.

4.3.9. Annexin V-FITC/Propidium iodide

The Annexin V-FITC/propidium iodide dual staining assay has been carried out to quantify the percentage of apoptotic cells. Briefly, A549 and MDA-MB-231 cells (1×10^6 /mL per well) were plated in six-well plates and allowed to grow for 24. Cells were treated with increasing concentrations of compound **9a** (0.5, 1 and 2 μ M) for 24 h and were collected by trypsinisation. The collected cells were washed twice with ice-cold PBS, then incubated with 200 μ L \times binding buffer containing 5 μ L Annexin V-FITC, and then in 300 μ L \times binding buffer containing 5 μ L Propidium iodide (PI) for 5 min at room temperature in the dark. After 15 min incubation, cells were analysed using BD-c6 accuri flow-cytometer.

Acknowledgements

C.P.K thanks RMIT and IICT-RMIT research centre for the research fellowship. R.S. acknowledges the support of Maxwell Eagle Cancer Endowment award for this research.

5. References

- [1] F. Hunziker, E. Fischer, J. Schmutz, 11-amino-5*H*-dibenzo[*b,e*][1,4] diazepine, *Helv. Chim. Acta*, 50 (1967) 1588-1599.
- [2] W.E. Coyne, J.W. Cusic, Anti-inflammatory dialkylaminoalkylureas, *J. Med. Chem.* 10 (1967) 541–546.
- [3] (a). R.D. Charan, G. Schlingmann, J.E. Janso, V. Bernan, X.D. Feng, G.T. Carter, Diazepinomicin a new antimicrobial alkaloid from a marine *Micromonospora* sp., *J. Nat. Prod.* 67 (2004) 1431-1433; (b) Y. Liao, P. DeBoer, E. Meier, H. Wikström, Synthesis and pharmacological evaluation of triflate-substituted analogues of clozapine, *J. Med. Chem.* 40(1997) 4146-4153; (c) B. Capuano, I.T. Crosby, E.J. Lloyd, D.A. Taylor, Synthesis and preliminary pharmacological evaluation of 4'-arylmethyl analogues of clozapine, *Aust. J. Chem.* 55 (2002) 565-576; (d) R. Mandrioli, L. Mercolini, M.A. Raggi, Benzodiazepinone metabolism: an analytical perspective, *Curr. Drug Metab.* 9 (2008) 827-844; (e) H.-Y. Zhao, G. Liu, A new strategy towards fused-pyridine heterocyclic scaffolds: Bischler-Napieralski-type cyclization, followed by sulfoxide extrusion reaction, *J. Comb. Chem.* 9 (2007) 1164-1176; (f) B. Petterson, V. Hasimbegovic, J. Bergman, One-pot Eschenmoserepisulfide contractions in DMSO: applications to the synthesis of fuligocandins A and B and a number of vinylogous amides, *J. Org. Chem.* 76 (2011) 1554-1561.
- [4] D.E. Thuston, D.S. Bose, Synthesis of DNA-interactive pyrrolo[2,1-*c*][1,4]benzodiazepines, *Chem. Rev.* 94 (1994) 433-465.
- [5] J.D. Albright, M.F. Feich, E.G.D. Santos, J.P. Dusza, F.W. Sum, A.M. Venkatesan, J. Coupet, P.S. Chan, X. Ru, H. Mazandarani, T. Bailey, 5-fluoro-2-methyl-*N*-[4-(5*H*-pyrrolo[2,1-*c*]-[1,4]benzodiazepine-10(11*H*)-ylcarbonyl)-3-chlorophenyl]benzamide: an

- orally active arginine vasopressin antagonist with selectivity for V₂ receptors, *J. Med. Chem.* 41 (1998) 2442-2444.
- [6] (a) H.J. Breslin, M.J. Kukla, D.W. Ludovici, R. Mohrbacher, W. Ho, M. Miranda, J.D. Rodgers, T.K. Hitchens, G. Leo, D.A. Gauthier, C.Y. Ho, M.K. Scott, E. De Clercq, R. Pauwels, K. Andries, M.A.C. Janssen, P.A. Janssen, Synthesis and anti-HIV activity of 4,5,6,7-tetrahydro-5-methylimidazo[4,5,1-jk][1,4]benzodiazepine-2(1*H*)-one (TIBO) derivatives, *J. Med. Chem.* 38 (1995) 771-793.;(b) A.J. Hansen, T. K. U. B. Jorgensen, Olsen, Patent WO2000032193, (2000); (c) M.E. Welsch, S.A. Snyder, B.R. Stockwell, Privileged scaffolds for library design and drug discovery, *Curr. Opin. Chem. Biol.* 14 (2010) 347-361.
- [7] (a) Y. Sanchez, C. Wong, R.S. Thoma, R. Richman, Z. Wu, H.P. Worms, S.J. Elledge, Conservation of the Chk1 checkpoint pathway in mammals: linkage of DNA damage to Cdk regulation through Cdc25, *Science* 277 (1997) 1497-1501.; b) Z. Xiao, Z. Chen, A.H. Gunasekera, T.J. Sowin, S.H. Rosenberg, S. Fesik, H. Zhang, *J. Biol. Chem.* 278 (2003) 21767-21773.
- [8] L.A. Hasvold, L. Wang, M. Przytulinska, Z. Xiao, Z. Chen, W.-Z. Gu, P.J. Merta, J. Xue, P. Kovar, H. Zhang, C. Park, T.J. Sowin, S.H. Rosenberg, N.-H. Lin, Investigation of novel 7,8-disubstituted-5,10-dihydro-dibenzo-[*b,e*][1,4]dibenzepin-11-ones as potent Chk1 inhibitors, *Bioorg. Med. Chem. Lett.* 18 (2008) 2311-2315.
- [9] (a) H. Gourdeau, J.B. McAlpine, M. Ranger, B. Simard, F. Berger, F. Beaudry, Identification, characterization and potent antitumor activity of ECO-4601, a novel peripheral benzodiazepine receptor ligand, *Cancer Chemother. Pharmacol.* 61 (2008) 911-921.;(b) B. O. Bachmann, J.B. McAlpine, E. Zazopoulos, C.M. Farnet, M. Pirae, WO 2004/065591 A1, Aug 5, (2004).; c) B.O. Bachmann, J.B. McAlpine, M. Pirae, U.S. 7,101,872 B2, Sept 5, (2006).

- [10] J.B. McAlpine, A.H. Banskota, R.D. Charan, G.Schlingmann, E. Zazopoulos, M. Pirae, J. Janso, V.S. Bernan, M. Aouidate, C.M. Farnet, X. Feng, Z. Zhao, G.T. Carter, Biosynthesis of diazepinomicin/ECO-4601, a *Micromonospora* secondary metabolite with a novel ring system, *J. Nat. Prod.* 71 (2008) 1585-1590.
- [11] V. Rambabu, S. Vijayakumar, In vitro cytotoxicity perspective of diazepinomicin (ECO-4601) on human hepatoma cell line (HEPG2), *Biomedicine & Aging Pathology* 4 (2014) 65-70.
- [12] B.B. Mishra, V.K. Tiwari, Natural products: an evolving role in future drug discovery, *Eur. J. Med. Chem.* 46 (2011) 4769-4807.
- [13] A. Kamal, A.V. SubbaRao, M.V. Vishnuvardhan, T. Srinivas Reddy, K. Swapna, C. Bagul, N.V. Subba Reddy, V. Srinivasulu, Synthesis of 2-anilinopyridyl-triazole conjugates as antimetabolic agents, *Org. Biomol. Chem.* 13 (2015) 4879-4895.
- [14] (a) M.J. Soltis, H.J. Yeh, K.A.N. Cole, Whittaker, R.P. Wersto, E.C. Kohn, Identification and characterization of human metabolites of CAI [5-amino-1-(4'-chlorobenzoyl-3,5-dichlorobenzyl)-1,2,3-triazole-4-carboxamide], *Drug Metab. Dispos.* 24 (1996) 799-806.;
b) L.S. Kallander, Q. Lu, W. Chen, T. Tomaszek, G. Yang, D. Tew, T.D. Meek, G.A. Hofmann, C.K. Schulz-Pritchard, W.W. Smith, C.A. Janson, M.D. Ryan, G.-F. Zhang, K.O. Johanson, R.B. Kirkpatrick, T.F. Ho, P.W. Fisher, M.R. Mattern, R.K. Johnson, M.J. Hansbury, J.D. Winkler, K.W. Ward, D.F. Veber, S.K. Thompson, 4-aryl-1,2,3-triazole: a novel template for a reversible methionine aminopeptidase 2 inhibitor, optimised to inhibit angiogenesis in vivo, *J. Med. Chem.* 48 (2005) 5644-5647.
- [15] (a) M.P. Zavelevich, L.M. Kuiava, V.F. Chekhun, D.Y. Blokhin, A.S. Kiselyov, M.N. Semenova, V.V. Semenov, Synthesis and Antiproliferative activity of conformationally restricted 1,2,3-triazole analogues of combretastatins in the sea urchin embryo model and against human cancer cell lines, *Bioorg. Med. Chem.* 22 (2014) 738-755.; (b) J.A. Stefely,

- R. Palchaudhuri, P.A. Miller, R.J. Peterson, G.C. Moraski, P.J. Hergenrother, M.J. Miller, *N*-((1-benzyl-1H-1,2,3-triazol-4-yl)arylamide as a new scaffold that provides rapid access to antimicrotubule agents: synthesis and evaluation of antiproliferative activity against select cancer cell lines, *J. Med. Chem.* 53 (2010) 3389-3395.
- [16] W.S. Horne, M.K. Yadav, C.D. Stout, M.R. Ghadiri, Heterocyclic peptide backbone modifications in an α -helical coiled coil *J. Am. Chem. Soc.* 126 (2004) 15366-15367.
- [17] R.P. Giani, M. Borsa, E. Parini, G.C. Tonon, A new facile synthesis of 11-oxo-10,11-dihydro-5*H*-dibenzo[*b,e*][1,4]diazepines, *Synthesis*, 5 (1985) 550-552.
- [18] L. Wang, G.M. Sullivan, L.A. Hexamer, L.A. Hasvold, R. Thalji, M. Przytulinska, Z.F. Tao, G. Li, Z. Chen, Z. Xiao, W.Z. Gu, J. Xue, M.H. Bui, P. Merta, P. Kovar, J. Bouska, H. Zhang, C. Park, K.D. Stewart, H.L. Sham, T.J. Sowin, S.H. Rosenberg, N.H. Lin, Design, synthesis, and biological activity of 5,10-dihydro-dibenzo[*b,e*][1,4]diazepin-11-one-based potent and selective Chk-1 inhibitors, *J. Med. Chem.* 50 (2007) 4162-4176.
- [19] S. Lu, H. Alper, Intramolecular carbonylation reactions with recyclable palladium-complexed dendrimers on silica: synthesis of oxygen, nitrogen, or sulphur-containing medium ring fused heterocycles, *J. Am. Chem. Soc.* 127 (2005) 14776-14784.
- [20] R.A. Bunce, J.E. Schammerhorn, Dibenzo-fused seven-membered nitrogen heterocycles by a tandem reduction-lactamization reaction, *J. Heterocycl. Chem.* 43 (2006) 1031-1035.
- [21] X. Diao, L. Xu, W. Zhu, Y. Jiang, H. Wang, Y. Guo, D. Ma, The *N*-aryl aminocarbonyl *ortho*-substituent effect in Cu-catalysed aryl amination and its application in the synthesis of 5-substituted 11-oxo-dibenzodiazepines, *Org. Lett.* 13 (2011) 6422-6425.
- [22] D. Tsvetikhovskiy, S.L. Buchwald, Concise palladium-catalyzed synthesis of dibenzodiazepines and structural analogues, *J. Am. Chem. Soc.* 133 (2011) 14228-14231.

- [23] T.H. Al-Tel, R. A. Al-Qawasmeh, M.F. Schmidt, A. Al-Aboudi, S.N. Rao, S.S. Sabri, W. Voelter, Rational design and synthesis of potent dibenzazepne motifs as β -secretase inhibitors, *J. Med. Chem.* 52 (2009) 6484-6488.
- [24] Y. Li, C. Zhan, B. Yang, X. Cao, C. Ma, A one pot transition-metal-free tandem process to 1,4-benzodiazepine scaffolds, *Synthesis*,45 (2013)111-117.
- [25] X. Li, L. Yang, X. Zhang, D. Zhang-Negrerie, Y. Du, K. Zhao, Construction of 1,4-benzodiazepine skeleton from 2-(arylamino)benzamides through $\text{PhI}(\text{OAc})_2$ -mediated oxidative C-N bond formation, *J. Org. Chem.* 79 (2014) 955-962.
- [26] Q.Y. Zhang, X.J. Wang, Y.L. Tian, J.G. Qi, C. Li, D.L. Yin, One pot synthesis of dibenzodiazepinones via CuI catalysis in ethylene glycol, *Chinese Chem. Lett.* 2013, 24, 825-828.
- [27] K. Feng, M. Lv, S. Liu, J. Wang, X. Zhao, S. You, J. Li, H. Cao, X. Guo, Synthesis and *in vitro* antibacterial activity of gemifloxacin derivatives containing a substituted benzyloxime moiety, *Eur. J. Med. Chem.*, 55 (2012) 125-136.
- [28] N.A Franken, H.M. Rodermond, J. Stap, J. Haveman, C. van Bree, Clonogenic assay of cells *in vitro*, *Nat. Protoc.* 1 (2006) 2315-2319.
- [29] L.G. Rodriguez, X. Wu, J. L. Guan, Wound healing assay, *Methods Mol. Biol.* 294 (2005) 23-29.
- [30] S. Fulda, Tumor resistance to apoptosis, *Int. J. Cancer* 124 (2009) 511-515.
- [31] J.C. Reed, Apoptosis-based therapies, *Nat. Rev. Drug Disc.* 1 (2002) 111-121.
- [32] X.D. Wang, Expanding the role of mitochondria in apoptosis, *Genes Dev.* 15 (2001) 2922-2933.
- [33] R.D. Miao, Y. Han, L.Z. An, J.B. Yang, Q. Wang, Seleno-podophyllotoxin derivatives induce hepatoma SMMC-7721 cell apoptosis through bax pathway, *Cell Biol. Int.* 32 (2008) 217-223.

- [34] (a) Y. Sánchez, G.P. Simón, E. Calviño, E. de Blas, P. Aller Curcumin stimulates reactive oxygen species production and potentiates apoptosis induction by the antitumor drugs arsenic trioxide and lonidamine in human myeloid leukaemia cell lines, *J. Pharmacol. Exp. Ther.*, 335 (2010) 114-123. b) K. Liu, D. Zhang, J. Chojnacki, Y. Du, H. Fu, S. Grant, S. Zhang, Design and biological characterisation of hybrid compounds of curcumin and thalidomide for multiple myeloma, *Org. Biomol. Chem.*, 11 (2013) 4757-4763.
- [35] D. Trachootam, J. Alexandre, P. Huang, *Nat. Rev. Drug Discovery* 8 (2009) 579-591.

Tables, Figures and Schemes captions

Table 1. Anti-proliferative activities ^a(IC₅₀-μM) of the 5,10-Dihydro-11*H*-dibenzo[*b,e*][1,4]diazepin-11-one and derivatives (**1,7** and **9a-k**).

Figure 1. Other Dibenzodiazepinones therapeutic compounds

Figure 2. Retrosynthetic routes I to VIII providing the medicinal dibenzodiazepine scaffold

Figure 3. Effect of compound **9a** on the colony formation ability of A549 and MDA-MB-231 cells.

Figure 4. Effect of compound **9a** on A549 and MDA-MB-231 cells migration *in vitro*. A549 and MDA-MB-231 cells were treated with **9a** and artificial wounds were induced with 200 μL pipette. The edges of wound were captured immediately (0 h), 24 and 48 h after respective treatments. Images were captured using a fluorescence microscope (Nikon).

Figure 5. Effect of compound **9a** on A549 and MDA-MB-231 cell cycle arrest. Cells were treated with **9a** and harvested after 24 h. The cells were fixed with ethanol, stained with propidium iodide and analyzed by BD-C6 accuri flow-cytometer. For each sample, 10,000 cells were used for sorting.

Figure 6. Compound **9a** induced nuclear morphological changes of A549 and MDA-MB-231 cells. Images were captured by a fluorescence microscope (Nikon).

Figure 7. Compound **9a** induced loss of mitochondrial membrane potential ($\Delta\Psi_m$) in A549 and MDA-MB-231 cells analysed using Rhodamine-123 staining. The loss in intensity of fluorescence was measured by spectrofluorometer. Data are mean \pm SD from three independent experiments.

Figure 8. Effect of compound **9a** on intracellular levels of ROS. **a)** A549 and MDA-MB-231 cells were treated with different concentrations of **9a** (0.5, 1 and 2 μ M) for 48 h and stained with carboxy-DCFDA. Images were captured by a fluorescence microscope (Nikon). **b)** Quantitative estimation of ROS was carried out fluorimetrically using an excitation wavelength of 485 nm and an emission wavelength of 535 nm.

Figure 9. Annexin V- FITC/propidium iodide dual staining assay. A549 cells were treated with increased concentrations of compound **9a** (0.5, 1 and 2 μ M) and stained with Annexin V-FITC and propidium iodide. 10000 cells from each sample were analysed by flow-cytometry. The percentage of cells positive for Propidium Iodide and/or Annexin V-FITC is reported inside the quadrants. Cells in the Lower left quadrant (Q1-LL: AV-/PI-) : Live cells, lower right quadrant (Q1-LR: AV+/PI-) : Early apoptotic cells, upper right quadrant (Q1-UR: AV+/PI+) Late apoptotic, upper left quadrant (Q1-UL: AV-/PI+) : necrotic cells.

Scheme 1. Synthesis of dibenzodiazepinone-triazole analogues. Reagents and conditions: (a) CuI, K₃PO₄, ethyleneglycol, 100 °C, 5 h, 50%; (b) *n*-BuLi, propargylbromide, -20 °C to RT, 4 h, 72%; (c) **8a-k**, CuSO₄·5H₂O, sodium ascorbate, *t*-BuOH/H₂O (1:1), RT, 12 h, 61-90%.

Table 1. Anti-proliferative activities ^a(IC₅₀- μ M) of the 5,10-Dihydro-11*H*-dibenzo[*b,e*][1,4]diazepin-11-one and derivatives (**1**, **7** and **9a-k**).

Compound	PC-3 ^b	A549 ^c	U87MG ^d	MCF-7 ^e	MDA-MB-231 ^e
1	41.89 \pm 2.7	37.10 \pm 1.3	8.97 \pm 0.9	>50	>50
7	0.98 \pm 0.3	19.01 \pm 3.7	22.19 \pm 0.8	7.63 \pm 1.3	16.51 \pm 1.3
9a	4.21 \pm 0.6	0.71 \pm 0.2	6.97 \pm 2.1	7.29 \pm 0.8	0.73 \pm 0.2
9b	>50	47.86 \pm 2.7	32.85 \pm 1.6	0.93 \pm 0.5	42.62 \pm 3.9
9c	0.47 \pm 0.08	>50	39.39 \pm 1.9	0.65 \pm 0.1	1.52 \pm 0.3
9d	17.28 \pm 1.1	26.68 \pm 0.4	37.72 \pm 0.6	>50	4.08 \pm 0.9
9e	8.63 \pm 1.0	11.32 \pm 0.5	48.21 \pm 2.7	5.27 \pm 0.9	>50
9f	7.21 \pm 0.8	8.37 \pm 1.0	2.06 \pm 0.5	4.12 \pm 0.09	3.53 \pm 0.1
9g	1.12 \pm 1.2	4.97 \pm 0.9	24.32 \pm 1.4	39.01 \pm 0.8	2.31 \pm 0.5
9h	>50	8.78 \pm 1.11	1.78 \pm 1.3	10.26 \pm 0.8	0.43 \pm 0.8
9i	>50	13.30 \pm 0.5	31.21 \pm 1.0	7.48 \pm 0.7	3.50 \pm 0.6
9j	10.67 \pm 1.2	10.70 \pm 1.0	13.48 \pm 0.6	17.78 \pm 0.5	10.19 \pm 0.8
9k	>50	>50	>50	29.61 \pm 1.3	>50
5-FU^f	1.44 \pm 0.3	3.47 \pm 0.9	3.61 \pm 0.5	nd	nd

^a 50% inhibitory concentration and mean \pm SD of three individual experiments performed in triplicate; ^b prostate cancer; ^c lung cancer; ^d glioblastoma and ^e breast cancer cells; ^f 5-Fluorouracil was included as reference standard; nd not determined.

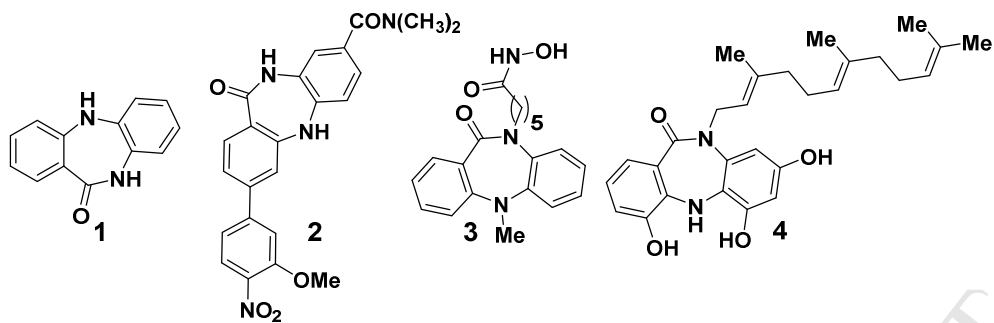


Figure 1. Other Dibenzodiazepinones therapeutic compounds

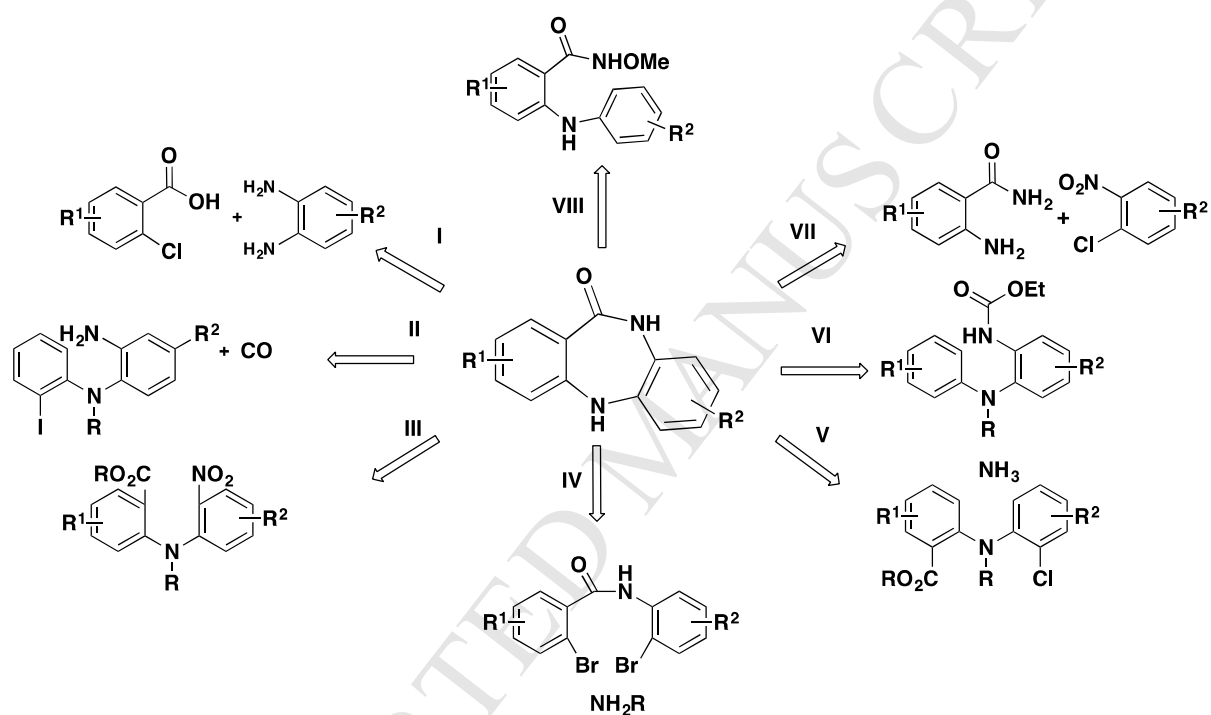


Figure 2. Retrosynthetic routes I to VIII providing the medicinal dibenzodiazepine scaffold

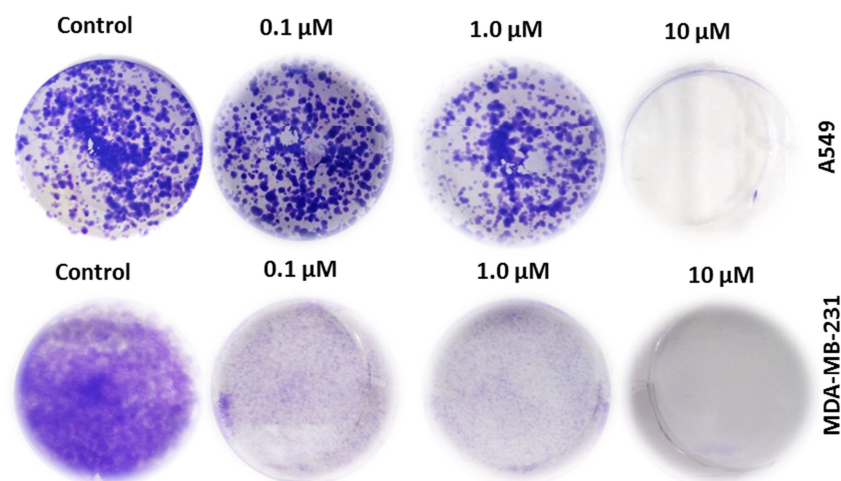


Figure 3. Effect of compound **9a** on the colony formation ability of A549 and MDA-MB-231 cells.

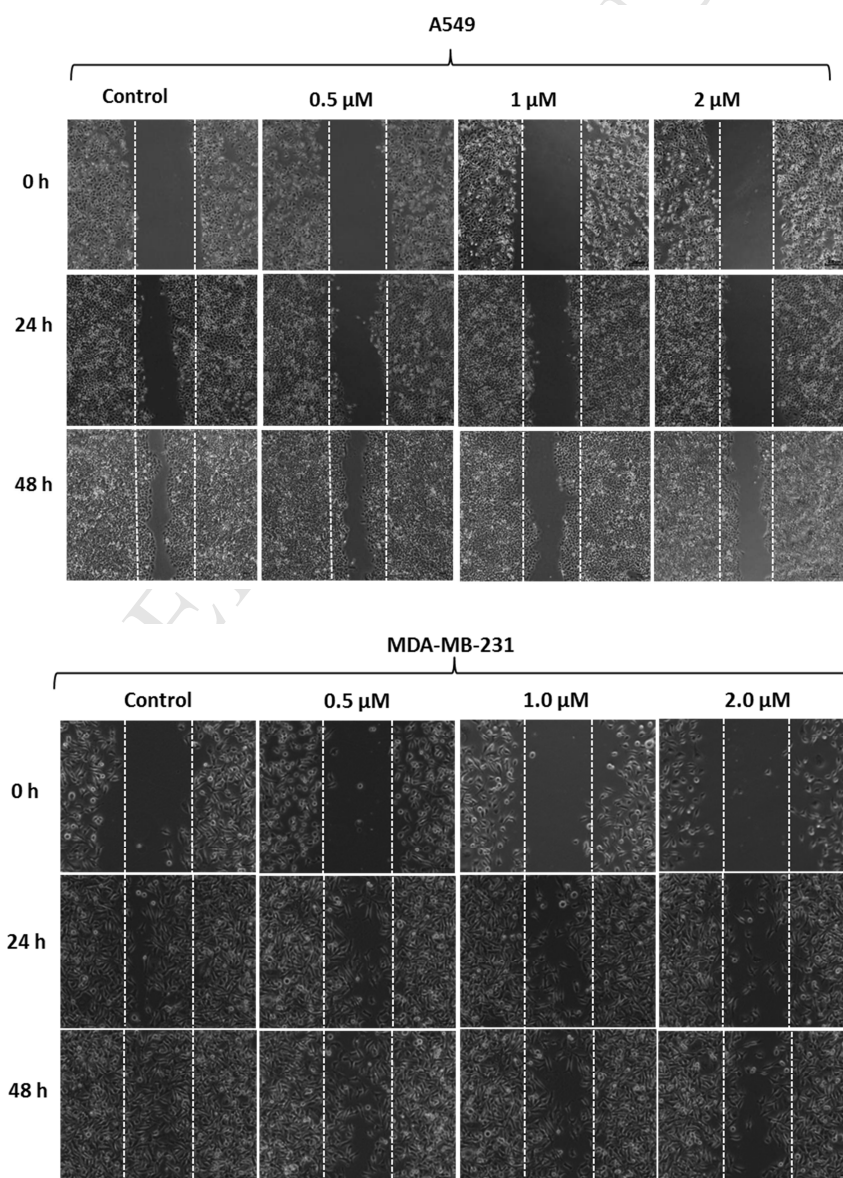


Figure 4. Effect of compound **9a** on A549 and MDA-MB-231 cells migration *in vitro*. A549 and MDA-MB-231 cells were treated with **9a** and artificial wounds were induced with 200 μ L pipette. The edges of wound were captured immediately (0 h), 24 and 48 h after respective treatments. Images were captured using a fluorescence microscope (Nikon).

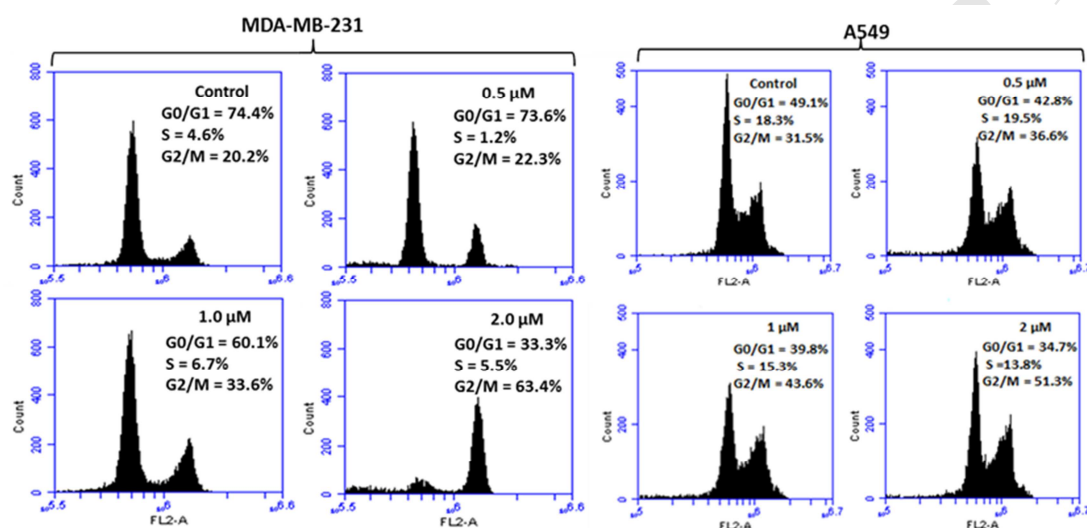


Figure 5. Effect of compound **9a** on A549 and MDA-MB-231 cell cycle arrest. Cells were treated with **9a** and harvested after 24 h. The cells were fixed with ethanol, stained with propidium iodide and analyzed by BD-C6 accuri flow-cytometer. For each sample, 10,000 cells were used for sorting.

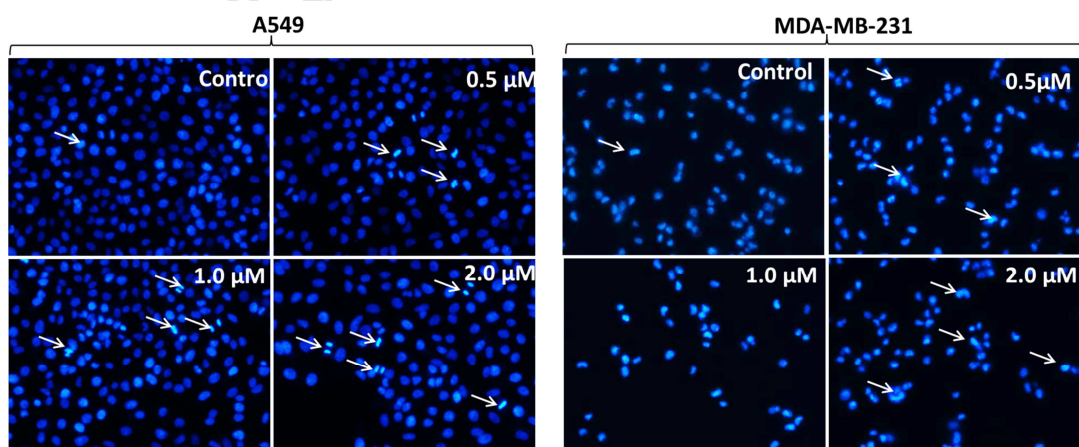


Figure 6. Compound **9a** induced nuclear morphological changes of A549 and MDA-MB-231 cells. Images were captured by a fluorescence microscope (Nikon).

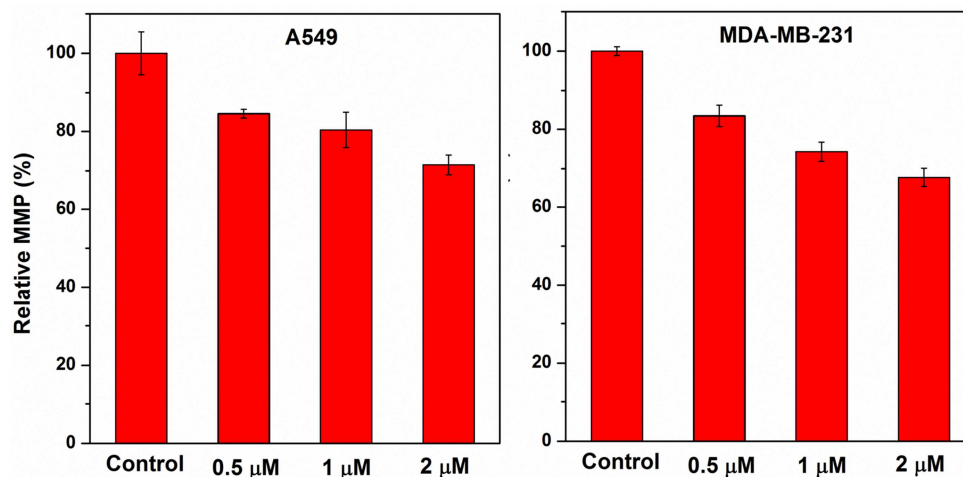
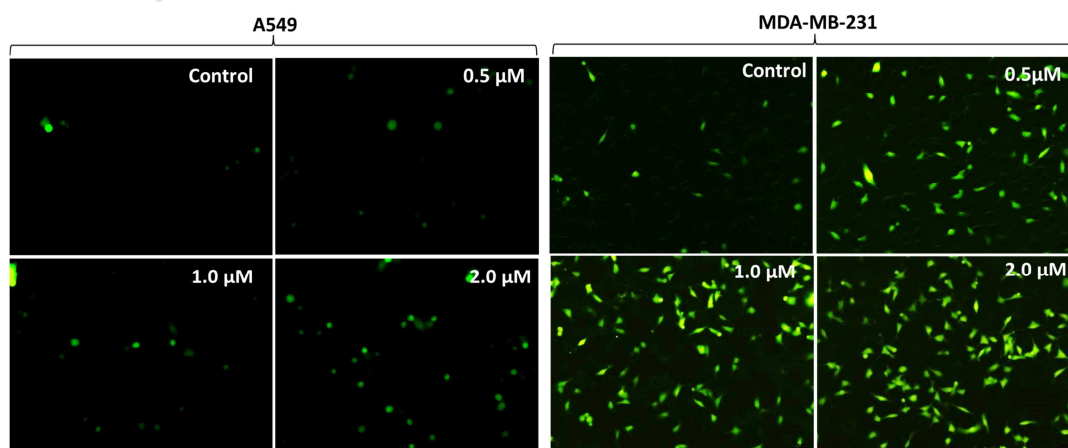


Figure 7. Compound **9a** induced loss of mitochondrial membrane potential ($\Delta\Psi_m$) in A549 and MDA-MB-231 cells analysed using Rhodamine-123 staining. The loss in intensity of fluorescence was measured by spectrofluorometer. Data are mean \pm SD from three independent experiments.

a)



b)

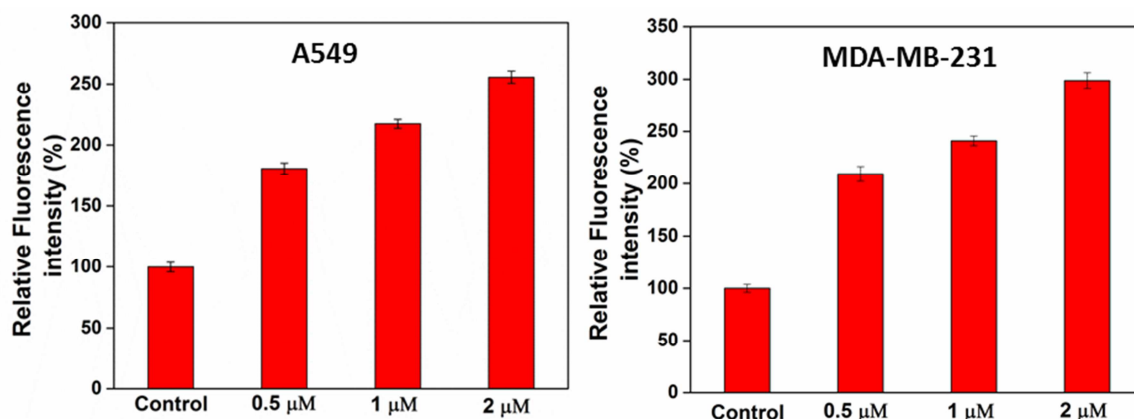


Figure 8. Effect of compound **9a** on intracellular levels of ROS. **a)** A549 and MDA-MB-231 cells were treated with different concentrations of **9a** (0.5, 1 and 2 μM) for 48 h and stained with carboxy-DCFDA. Images were captured by a fluorescence microscope (Nikon). **b)** Quantitative estimation of ROS was carried out fluorimetrically using an excitation wavelength of 485 nm and an emission wavelength of 535 nm.

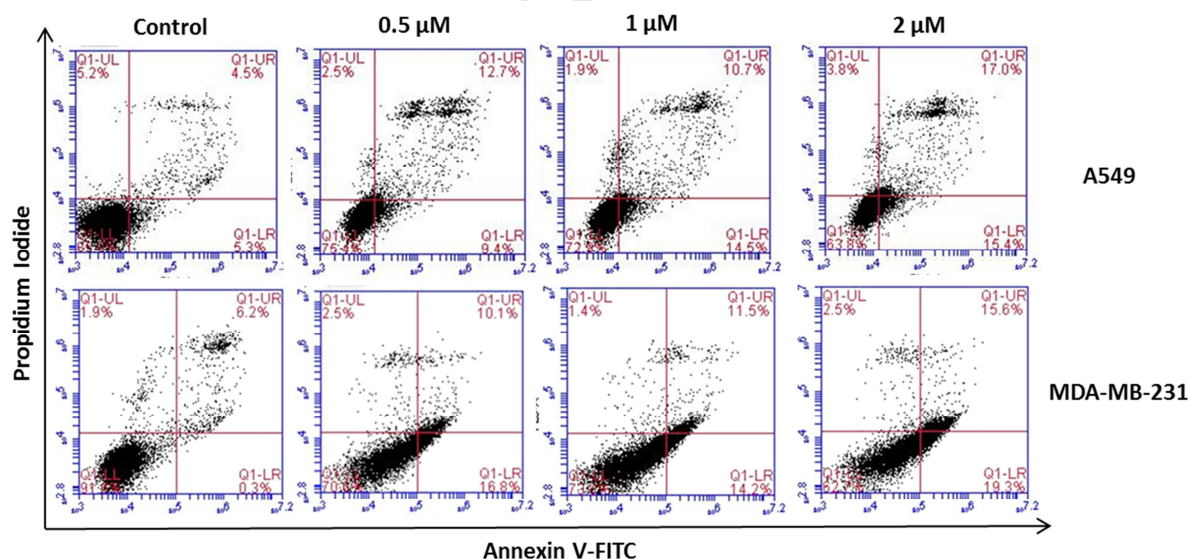
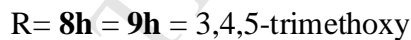
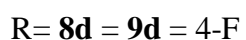
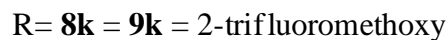
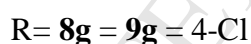
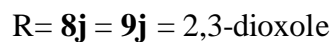
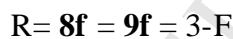
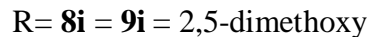
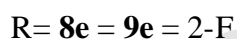
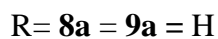
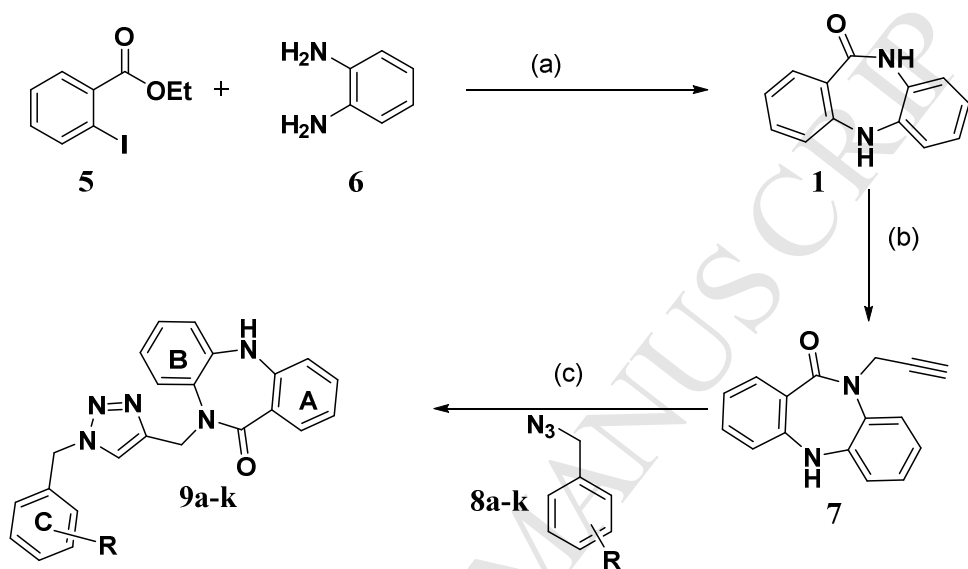


Figure 9. Annexin V- FITC/propidium iodide dual staining assay. A549 cells were treated with increased concentrations of compound **9a** (0.5, 1 and 2 μM) and stained with Annexin V-FITC and propidium iodide. 10000 cells from each sample were analysed by flow-

cytometry. The percentage of cells positive for Propidium Iodide and/or Annexin V-FITC is reported inside the quadrants. Cells in the Lower left quadrant (Q1-LL: AV-/PI-): Live cells, lower right quadrant (Q1-LR: AV+/PI-): Early apoptotic cells, upper right quadrant (Q1-UR: AV+/PI+) Late apoptotic, upper left quadrant (Q1-UL: AV-/PI+): necrotic cells.



Scheme 1. Synthesis of dibenzodiazepinone-triazole analogues. Reagents and conditions: (a) CuI, K_3PO_4 , ethyleneglycol, 100 °C, 5 h, 50%; (b) *n*-BuLi, propargylbromide, -20 °C to RT, 4 h, 72%; (c) **8a-k**, $\text{CuSO}_4 \cdot 5\text{H}_2\text{O}$, sodium ascorbate, *t*-BuOH/ H_2O (1:1), RT, 12 h, 61-90%.

Highlights

- The anticancer applications of the readily synthesised dibenzodiazepinone-triazole scaffold is promising
- Studies with compound **9a** on lung and breast cancer lines revealed its anticancer activity (*in vitro*) occurred in the G2/M phase of the cell cycle
- Furthermore this compound is also an effective apoptosis inducing agent
- Evidence for the presence of elevated reactive oxygen species was found